Beam Selection for Ambient Backscatter Communication in Beamspace mmWave Symbiotic Radio

Muhammad Bilal Janjua, *Student Member, IEEE*, Hasan Tahir Abbas, *Senior Member, IEEE*,
Khalid A. Qaraqe, *Senior Member, IEEE*, and Hüseyin Arslan, *Fellow, IEEE*

Abstract—The Internet of Things revolution has profoundly impacted wireless communication systems. Access to high data rates is now just as important as low power operation. The use of incident millimeter-wave (mmWave) signals for ambient backscatter communication (AmBC) has shown significant promise for delivering high data rates. However, due to channel sparsity, incident signal availability to backscatter devices (BDs) at mmWave is erratic. In order to address the incident signal inaccessibility problem and enable high data-rate AmBC, this letter presents an efficient beam selection method in the beamspace millimeter-wave symbiotic radio system. The proposed method improves the overall system's sum-rate performance by up to 30% while ensuring signal accessibility to BDs.

Index Terms—Ambient backscatter communication, mmWave symbiotic radio, beam selection, beamspace MIMO.

I. INTRODUCTION

WE ARE witnessing great technological strides in the widespread adoption of Internet of Things (IoT). As a result, more and more devices are going online, and the demand for the electromagnetic spectrum is now more than ever. In recent years, we have witnessed the inclusion of IoT in various systems such as healthcare, education, industry, agriculture, transportation, and so on [1]. Until now, IoT devices are supposed to have low data rates and energy efficiency requirements. However, with the development of extended reality, a high data rate has become another critical requirement, particularly in the case of wearable devices, e.g., XR glasses [2].

Muhammad Bilal Janjua is with the Department of Electrical and Electronics Engineering, Istanbul Medipol University, 34810 Istanbul, Turkey, and also with the Department of Electrical and Computer Engineering, Texas A&M University at Qatar, Doha, Qatar (e-mail: muhammad.janjua@std.medipol.edu.tr).

Hasan Tahir Abbas is with the James Watt School of Engineering, University of Glasgow, G12 8QQ Glasgow, U.K. (e-mail: hasan.abbas@glasgow.ac.uk).

Khalid A. Qaraqe is with the Department of Electrical and Computer Engineering, Texas A&M University at Qatar, Doha, Qatar (e-mail: khalid.qaraqe@qatar.tamu.edu).

Hüseyin Arslan is with the Department of Electrical and Electronics Engineering, Istanbul Medipol University, 34810 Istanbul, Turkey (e-mail: huseyinarslan@medipol.edu.tr).

Digital Object Identifier 10.1109/LWC.2023.3235104

Ambient backscatter communication (AmBC) is considered a revolutionary energy-efficient technology for sixth-generation (6G) and beyond wireless systems [3]. Unlike conventional radio systems, AmBC system uses ambient radio-frequency (RF) signals of existing wireless systems as a carrier for communication. Although AmBC system can substantially enhance the energy efficiency, its dependency on ambient signals poses a great question regarding its reliability. Recently, a symbiotic radio (SRad) is proposed to enhance the reliability of AmBC through a cooperative resource sharing with existing wireless systems [4].

On the other hand, millimeter-wave (mmWave) frequency bands offer large bandwidths and provide very high data rates and long-range communication with the support of massive multiple-input multiple-output (MIMO) systems. Although these technologies are the critical enablers of fifth-generation (5G) and beyond wireless systems, their full potential has not been experienced yet due to significant energy consumption and hardware cost that comes from RF chains required to support a massive number of antennas. To overcome these problems, a beamspace MIMO system has been proposed to exploit the channel sparsity at mmWave frequency. In addition, different beam-selection methods are applied to select the beams with high path gains to reduce the number of RF chains and enhance the energy efficiency gains [5], [6]. For instance, a maximum magnitude (MM) beam-selection method captures the maximum fraction of power from the channel by selecting dominant beams and leaving the weak ones. However, the conventional beam selection schemes are not suitable in the case of the mmWave AmBC system since backscatter devices (BDs) may exist in beams with low path gains and be out of coverage.

SRad combines the benefits of mmWave and AmBC to achieve low-power high data rate communication. In [7], a mmWave SRad with single BD is proposed to achieve high data rate in AmBC. In particular, a joint hybrid and passive beamforming approach is used at transmitter and BD. Unlike this letter, we aim to provide the RF signal accessibility to BDs while selecting the beams for a user in mmWave SRad system.

In this letter, our main contributions to the literature for the development of mmWave SRad are as follows,

- To the best of the authors' knowledge, this is the first study that addresses the RF signal inaccessibility issue for AmBC in the sparse mmWave system. In particular, we develop a SRad to enable cooperation among AmBC and existing mmWave systems to ensure signal accessibility to BDs.

- This letter leverages the beamspace MIMO and proposes a beam selection scheme considering BDs as a part of the mmWave system to enhance the sum-rate performance of SRad.
- Assuming perfect channel state information (CSI), the performance of the proposed scheme is compared with the conventional MM based beam selection scheme, showing up to 30% sum-rate enhancement with the beam-selection and the selection of the paths with BDs and ordinary scatterers.

In addition to the contributions mentioned above, our results can be used as a benchmark for future studies.

II. mmWave SRad Modelling

A. System Model

We consider a SRad comprising an AmBC system with a mmWave MIMO communication system. A beamspace hybrid analog-digital beamforming architecture at the mmWave MIMO system is assumed consisting of N_{Tx} and N_{Rx} antenna elements at transmitter (Tx) and receiver (Rx), respectively [6], [8]. With each antenna element having a uniform radiation in all directions, the array steering vectors at Rx $\mathbf{a}_R(\phi_R)$ and Tx $\mathbf{a}_T(\phi_T)$ as a function of angle-of-departure (AoD) and angle-of-arrival (AoA) are given by

$$\mathbf{a}_{Rx}(\phi_R) = \left[1, e^{-j2\pi\varphi_R}, \ldots, e^{-j2\pi\varphi(N_{Rx}-1)}\right]^T \quad (1)$$

and

$$\mathbf{a}_{Tx}(\phi_T) = \left[1, e^{-j2\pi\phi_T}, \ldots, e^{-j2\pi\phi(N_{Tx}-1)}\right]^T. \quad (2)$$

where $\varphi = \frac{\Omega\sin(\phi)}{\lambda}$ represents the normalized spatial beamforming angles according to physical direction of AoA(AoD) $\phi_T(\phi_R) \in [-\frac{\pi}{2}, \frac{\pi}{2}]$. Ω denotes the antenna element spacing with $\Omega = \lambda/2$, where λ is the wavelength. Tx transmits N_s data streams to the Rx, where $N_s < N_{Rx} < N_{Tx}$.

AmBC system consists of N_b single antenna passive BDs, i.e., IoT devices, which also send their data to Rx by modulating the incident RF signals/beams generated by Tx. The modulation at BD is performed by changing the load impedance and switching the antenna into reflecting and non-reflecting states. Specifically, the backscatter modulation at b-th BD with antenna switching can be expressed by the antenna reflection coefficient $\Gamma_b^{(c)}$ defined as,

$$\Gamma_b^{(c)} = \frac{Z_{L,b}^{(c)} - Z_{a,b}^*}{Z_{L,b}^{(c)} + Z_{a,b}}, \quad (3)$$

where $Z_{L,b}^{(c)}$ is the load impedance, $Z_{a,b}$ is the antenna impedance of b-th BD, $*$ is the complex conjugate, and $c = 1, 2$ are the switch states. We assume the information bit zero '0' is represented by load impedance matching with the antenna impedance, i.e., $Z_{L,b}^{(c)} = Z_{a,b}^*$, when antenna absorbs the RF signal. On the other hand, the information bit one '1' is represented by impedance mismatch, i.e., $Z_{L,b}^{(c)} \neq Z_{a,b}^*$, when antenna completely reflects the RF signal. $\Gamma_b^{(c)} \in [0, 1]$ controls the backscattered signal power at BD.
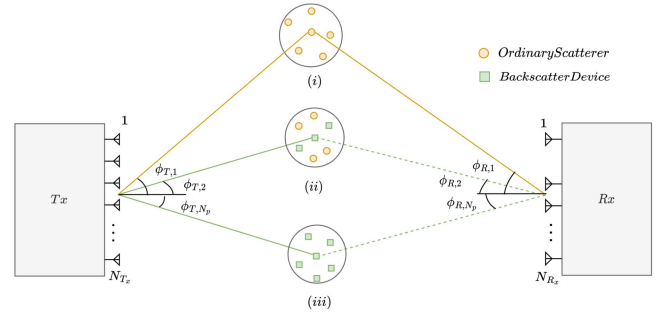

Fig. 1. The mmWave MIMO SRad system model with three different types of scatterers in the cluster: i) ordinary scatterers; ii) BDs in ordinary scatterers; iii) only BDs.

B. Channel Model

We assume a sparse narrowband mmWave MIMO communication channel with only a few scattering clusters[1] due to propagation characteristics of signals in mmWave frequencies [9]. In contrast to the traditional mmWave MIMO system, scatterers can either be common scattering objects or BDs in SRad. As a result, we divide the scattering clusters into three categories, as depicted in Fig. 1. Similar to normal clusters represented in mmWave MIMO systems, the first cluster type has just ordinary scatterers as outside sources. Ordinary scatterers and BDs exist in the second cluster type, but BDs are the only objects in the third cluster type. However, due to the high channel sparsity, there is only one path from either a BD or an ordinary scatterer in each cluster at mmWave bands. Thus, channel between Tx and Rx is modelled according to the extended Saleh-Valenzuela model [10],

$$\mathbf{H} = \sqrt{\frac{N_{Rx}N_{Tx}}{N_p}} \sum_{p=1}^{N_p} \alpha_p \mathbf{a}_{Rx}(\phi_{R,p})\mathbf{a}_{Tx}^H(\phi_{T,p}), \quad (4)$$

where $\mathbf{H} \in \mathbb{C}^{N_{Rx} \times N_{Tx}}$ represents the channel between Rx and Tx, α_p with $p = 1, 2, \ldots, N_p$, $\mathbf{a}_{Rx}(\phi_{R,p}) \in \mathbb{C}^{N_{Rx} \times 1}$, and $\mathbf{a}_{Tx}(\phi_{T,p}) \in \mathbb{C}^{N_{Tx} \times 1}$ are the complex path gain, steering vectors for AoA $\phi_{R,p}$ and AoD $\phi_{T,p}$ of the p-th path, respectively. Furthermore, uniform linear array (ULA) of antennas are considered at Tx and Rx in a horizontal placement, and $\phi_{R,p}$ and $\phi_{T,p}$ are azimuth AoA and AoD of the p-th path.

Since there can be ordinary scatterers or BDs in the paths (i.e., $p \in [b, l]$), we define $N_p = N_b + N_l$, where N_b, and N_l denote number of BDs and number of ordinary scatterers, respectively, which contribute to the N_p paths. In case there are no BDs, then $N_b = 0$ and $N_p = N_l$. Similarly, when there are only BDs, then $N_p = N_b$ and $N_l = 0$. In all three cases, contributing scatterers are assumed to be non-vanishing and exist in the far-field of Tx and Rx. Besides, the number of paths are less than number of antennas at Tx and Rx (i.e., $N_p \leq N_{RX} \leq N_{Tx}$). In our proposed system, each path between Tx and Rx represents a channel of a BD or an

---

[1]We consider the clusters generated from single-bounce reflections only.

ordinary scatterer, and (4) is rewritten as,

$$\mathbf{H} = \gamma \left(\sum_{b=1}^{N_b} \alpha_b \mathbf{a}_{Rx}(\phi_{R,b}) \mathbf{a}_{Tx}^H(\phi_{T,b}) \right.$$
$$\left. + \sum_{l=1}^{N_l} \alpha_l \mathbf{a}_{N_{Rx}}(\phi_{R,l}) \mathbf{a}_{N_{Tx}}^H(\phi_{T,l}) \right), \quad (5)$$

where $\gamma = \sqrt{\frac{N_{Rx} N_{Tx}}{N_b + N_l}}$ is the normalization factor. To describe the channel in a matrix form, (6) can also be written as,

$$\mathbf{H} = \mathbf{A}_{Rx} \Delta_{\mathcal{B}} \mathbf{A}_{Tx}^H + \mathbf{A}_{Rx} \Delta_{\mathcal{L}} \mathbf{A}_{Tx}^H$$
$$= \mathbf{H}_{\mathcal{B}} + \mathbf{H}_{\mathcal{L}} \quad (6)$$

where $\mathbf{A}_{Rx} = [\mathbf{a}_{Rx}(\phi_{R,1}), \ldots, \mathbf{a}_{Rx}(\phi_{R,N_p})]$ and $\mathbf{A}_{Tx} = [\mathbf{a}_{Tx}(\phi_{T,1}), \ldots, \mathbf{a}_{Tx}(\phi_{T,N_p})]$ are the array response matrices of Rx and Tx, respectively, $\Delta_{\mathcal{B}} = \gamma \ \text{diag}[\alpha_{11} \ \alpha_{bb} \ \alpha_{N_b N_b} \ 0_{11} \ 0_{N_l N_l}]$, and $\Delta_{\mathcal{L}} = \gamma \ \text{diag}[0_{11} \ 0_{bb} \ 0_{N_b N_b} \ \alpha_{11} \ \alpha_{N_l N_l}]$ are matrices consisting of the complex path gains of BDs and ordinary scatterers, respectively. Now to obtain the finite dimensionality of the mmWave massive MIMO system, we use a beamspace representation with fixed beamforming at Tx and Rx. Thus, the beamspace representation of channel $\mathbf{H}$ is described as [11],

$$\mathbf{H} = \sum_{i=1}^{N_{Rx}} \sum_{j=1}^{N_{Tx}} \tilde{H}(i,j) \mathbf{a}_{Rx}(\hat{\phi}_{R,i}) \mathbf{a}_{Tx}^H(\hat{\phi}_{T,j})$$
$$= \mathbf{U}_{Rx} \tilde{\mathbf{H}} \mathbf{U}_{Tx}^H \quad (7)$$

where $\mathbf{U}_{Tx}$ and $\mathbf{U}_{Rx}$ represents the discrete Fourier transform matrices at Tx and Rx, respectively, which can be defined as [12],

$$\mathbf{U}_t = \frac{1}{\sqrt{N_t}} \left[\mathbf{a}_t(\hat{\phi}_v) \right]. \quad (8)$$

$\mathbf{U}_t$ with $t \in \{Tx, Rx\}$ is a $N_t \times N_t$ unitary matrix with $\mathbf{U}_t^H \mathbf{U}_t = \mathbf{U}_t \mathbf{U}_t^H = \mathbf{I}_{N_t}$, and $\hat{\phi}_v = \frac{1}{N_t}(v - \frac{N_t+1}{2})$ for $v = 1, 2, \ldots, N_t$ are pre-defined spatial directions. The transformation of $\mathbf{H}$ into beamspace domain gives the sparse representation at the mmWave frequencies. Furthermore, the beamspace channel matrix is unitarily equivalent to the physical channel matrix, such that

$$\tilde{\mathbf{H}} = \mathbf{U}_{Rx}^H \mathbf{H} \mathbf{U}_{Tx}. \quad (9)$$

From $\tilde{\mathbf{H}}$, we can select the beams that contribute to BDs' paths to provide them signal accessibility and the beams for ordinary scatterers with high path gains.

C. Joint Receiver Design

Let $\mathbf{x}$ be the signal transmitted from Tx to Rx in the direction of BDs and ordinary scatterers. BD transmits its information signal $q_b \sim \mathcal{N}(0,1)$ by modulating the incident beam coming from Tx [13]. The signal transmitted by Tx also serves the BDs as an RF carrier. BDs modulate their data by switching antennas while ordinary scatterers only reflect the incident signal. The final received signal containing the

information of BD and Rx can be expressed in the antenna domain as,

$$\mathbf{y} = (\mathbf{H}_{\mathcal{B}} \mathbf{q} + \mathbf{H}_{\mathcal{L}}) \mathbf{x} + \mathbf{z}$$
$$= (\mathbf{A}_{Rx} \Delta_{\mathcal{B}}^{\mathbf{q}} \mathbf{A}_{Tx}^H + \mathbf{A}_{Rx} \Delta_{\mathcal{L}} \mathbf{A}_{Tx}^H) \mathbf{x} + \mathbf{z} \quad (10)$$

where $\mathbf{y} \in \mathbb{C}^{N_{Rx} \times 1}$ is the received signal vector, $\mathbf{x} \in \mathbb{C}^{N_{Tx} \times 1}$ is the signal vector transmitted by Tx, $\Delta_{\mathcal{B}}^{\mathbf{q}} = \text{diag}([\alpha_1 \Gamma_1^{(c)} q_1 \ \alpha_2 \Gamma_2^{(c)} q_2 \ \alpha_{N_b} \Gamma_{N_b}^{(c)} q_{N_b} \ 0_{11} \ 0_{N_l N_l}])$ represents the signal vector containing information of BDs' $\mathbf{q} \in \mathbb{R}^{N_b \times 1}$, and $\mathbf{z} \sim \mathcal{CN}(0, \sigma^2 \mathbf{I})$ represents the noise vector. The system model provided in (10) can be re-written in equivalent beamspace representation,

$$\tilde{\mathbf{y}} = \tilde{\mathbf{H}} \tilde{\mathbf{x}} + \tilde{\mathbf{z}}$$
$$= \mathbf{U}_{Rx}^H (\mathbf{H}_{\mathcal{B}} \mathbf{q} + \mathbf{H}_{\mathcal{L}}) \mathbf{U}_{Tx} \tilde{\mathbf{x}} + \tilde{\mathbf{z}}$$
$$= \mathbf{U}_{N_{Rx}}^H (\mathbf{A}_{Rx} \Delta_{\mathcal{B}}^{\mathbf{q}} \mathbf{A}_{Tx}^H + \mathbf{A}_{Rx} \Delta_{\mathcal{L}} \mathbf{A}_{Tx}^H) \mathbf{U}_{N_{Tx}} \tilde{\mathbf{x}} + \tilde{\mathbf{z}}$$
$$= (\tilde{\mathbf{H}}_{Rx,\mathcal{B}} \Delta_{\mathcal{B}}^{\mathbf{q}} \tilde{\mathbf{H}}_{Tx,\mathcal{B}} + \tilde{\mathbf{H}}_{Rx,\mathcal{L}} \Delta_{\mathcal{L}} \tilde{\mathbf{H}}_{Tx,\mathcal{L}}) \tilde{\mathbf{x}} + \tilde{\mathbf{z}},$$
$$= (\tilde{\mathbf{H}}_{\mathcal{B}} \mathbf{q} + \tilde{\mathbf{H}}_{\mathcal{L}}) \tilde{\mathbf{x}} + \tilde{\mathbf{z}}, \quad (11)$$

where $\tilde{\mathbf{y}} = \mathbf{U}_{N_{Rx}}^H \mathbf{y}$, $\tilde{\mathbf{x}} = \mathbf{U}_{N_{Tx}}^H \mathbf{x}$, and $\tilde{\mathbf{z}} = \mathbf{U}_{N_{Rx}}^H \mathbf{z}$, are the received signal, transmitted signal and noise vectors in the beamspace, respectively. $\tilde{\mathbf{H}}_{Tx,\mathcal{B}} (\tilde{\mathbf{H}}_{Tx,\mathcal{L}})$ represents beamspace channel matrix between Tx and BD (ordinary scatterers), and $\tilde{\mathbf{H}}_{Rx,\mathcal{B}} (\tilde{\mathbf{H}}_{Rx,\mathcal{L}})$ denotes the beamspace channel matrix between Rx and BDs (ordinary scatterers).

III. SIGNAL ACCESSIBILITY TO BDs THROUGH BEAM SELECTION AT TX AND RX

In this section, we present a beam selection scheme for ensuring signal accessibility to BDs at the Tx and Rx. Let us consider the MM beam selection, in which the dominant transmit and receive beams are selected from $\tilde{\mathbf{H}}$ to obtain a low-dimensional channel matrix, which is described as [14],

$$\overline{\mathbf{H}} = \left[\tilde{\mathbf{H}}(j,k) \right]_{j \in \mathcal{M}_{Rx}, k \in \mathcal{M}_{Tx}}, \quad (12)$$

where $\mathcal{M}_{Rx} = \{ j \in \mathcal{J}(N_{Rx}) : (j,k) \in \mathcal{M}_c \}$, $\mathcal{M}_{Tx} = \{ k \in \mathcal{K}(N_{Tx}) : (j,k) \in \mathcal{M}_c \}$, and $\mathcal{M}_c$ denotes the mask for the selection of dominant beams with a power difference of $\zeta \in [0,1]$ from the strongest beam, and it is defined as [8],

$$\mathcal{M}_c = \left\{ (j,k) : |\tilde{\mathbf{H}}(j,k)|^2 \geq \zeta \max_{j,k} |\tilde{\mathbf{H}}(j,k)|^2 \right\}. \quad (13)$$

This scheme provides a set of beams $s_c = |\mathcal{M}_c|$ with high gains that captures a fraction of channel power. Selecting the beams with dominant path-gain while ignoring others may lead to limited or no signal accessibility to some BDs, and AmBC may not be possible in this case. Therefore, the sparsity mask is redefined in the proposed scheme while considering the channel paths of BDs. Assuming the availability of perfect CSI,[2] we define $\mathbb{H}_{\mathcal{B}}$ and select the beams that provide signal

---

[2]The channel estimation can be performed in two stages. The DoD of the Tx-to-BD channel and DoA of the BD-to-Rx channel are estimated in the first stage. In the second stage, the estimated channel parameters are used to estimate cascaded channel TX-to-BD-to-Rx parameters, including complex path gains [15]. Similarly, for imperfect CSI, the method presented in [16] can be followed.

accessibility to BDs with MM

$$\mathbb{H}_{\mathcal{B}} = [\tilde{\mathbf{H}}_{\mathcal{B}}(j_b, k_b)]_{j_b \in \mathcal{M}_{Rx,b}, k_b \in \mathcal{M}_{Tx,b}}, \quad (14)$$

where $\mathcal{M}_{Rx,b} = \{j_b \in \mathcal{J}(N_{Rx}) : (j_b, b) \in \mathcal{M}_{\mathcal{B}}\}$, $\mathcal{M}_{Tx,b} = \{k_b \in \mathcal{K}(N_{Tx}) : (k_b, b) \in \mathcal{M}_{\mathcal{B}}\}$, and $\mathcal{M}_{\mathcal{B}}$ denotes the beam selection mask for BDs. To determine $\mathcal{M}_{\mathcal{B}}$, another sparsity mask $\mathcal{M}_b$ is defined for dominating beams at Tx and Rx covering b-th backscatter,

$$\mathcal{M}_b = \begin{Bmatrix} j_b : |\tilde{\mathbf{H}}_{Rx,\mathcal{B}}(j, b)|^2 = \max_{(j_b, b)} |\tilde{\mathbf{H}}_{Rx,\mathcal{B}}(j_b, b)|^2 \\ k_b : |\tilde{\mathbf{H}}_{Tx,\mathcal{B}}(k_b, b)|^2 = \max_{(k_b, b)} |\tilde{\mathbf{H}}_{Tx,\mathcal{B}}(k_b, b)|^2 \end{Bmatrix}$$
$$\mathcal{M}_{\mathcal{B}} = \bigcup_{b=1,\ldots,N_b} \mathcal{M}_b. \quad (15)$$

From $\mathcal{M}_{\mathcal{B}}$, a set of beams represented by $s_{\mathcal{B}} = |\mathcal{M}_{\mathcal{B}}|$ is selected that consists of beams which provide signal accessibility to BDs only. Furthermore, a final set of beams denoted by $s_F = |\mathcal{M}_F|$ is chosen by comparing $s_{\mathcal{B}}$ with s_c to select the high path gain beams correspond to Rx. By ensuring signal accessibility to BDs, $s_F = |\mathcal{M}_F|$ is described as

$$s_F = \begin{cases} s_c, & s_{\mathcal{B}} \subset s_c, \\ s_c \cup (s_{\mathcal{B}} - s_c) & s_{\mathcal{B}} \not\subset s_c. \end{cases} \quad (16)$$

After selecting the beams through the proposed scheme $\overline{\mathbf{H}}$ in (12) is redefined based on s_F and the received signal at Rx is given by

$$\tilde{\mathbf{y}} = \overline{\mathbf{H}}\tilde{\mathbf{x}} + \tilde{\mathbf{z}}; \quad \overline{\mathbf{H}} = \mathbb{H}_{\mathcal{B}} + \mathbb{H}_{\mathcal{L}}, \quad (17)$$

where $\mathbb{H}_{\mathcal{L}}$ represents the channel matrices corresponding to ordinary scatterers, and it is determined similar to $\mathbb{H}_{\mathcal{B}}$.

The major complexity of the proposed scheme comes from the number of beams selected at Tx and Rx. It is comparable to the complexity of conventional MM beam selection scheme, which is expressed as $\mathcal{O}(s_c)$ [8], [12]. Besides, the transceiver needs additional RF chains to provide signal accessibility. In the case selected beams do not cover all BDs, then the complexity is determined as $\mathcal{O}(s_F)$, where s_F is given in (16). However, the additional complexity brings the sum-rate performance improvement of the SRad system.

The performance of the proposed beam selection scheme is measured in terms of the achievable sum-rate. To simplify the notation, we will use $p \in \{b, l\}$ instead of b and l as defined in (4). Rx considers the signal of BDs as interference and obtains its sum-rate in the following manner,

$$R_{Rx} = \log_2 \det \left(\mathbf{I} + \frac{\rho|\beta|^2}{N_p} \mathbf{G}_{Rx}^H \overline{\mathbf{H}}\, \overline{\mathbf{H}}^H \mathbf{G}_{Tx} \mathcal{R}^{-1} \right) \quad (18)$$

where $\mathbf{G}_t = \beta \mathbf{F}_t = \beta[\mathbf{f}_{t,1}, \mathbf{f}_{t,p}, \ldots, \mathbf{f}_{t,N_p}]$ denotes the precoder for $t = Tx$ and filter matrix for $t = Rx$, respectively. In the case of linear transceivers, we use $\mathbf{F} = \overline{\mathbf{H}}$ as a matched filter. β satisfies the total power constraint as follows $\beta = \sqrt{\frac{\rho}{tr(\mathbf{F}_{Tx}^H \Delta_p \mathbf{F}_{Tx})}}$. $\mathcal{R}$ represents interference-plus-noise in the received signal, which is

$$\mathcal{R} = \sigma_n^2 + \frac{\rho|\beta|^2}{N_p} \mathbf{G}_{Rx}^H \mathbb{H}_{\mathcal{B}} \mathbb{H}_{\mathcal{B}}^H \mathbf{G}_{Tx}. \quad (19)$$
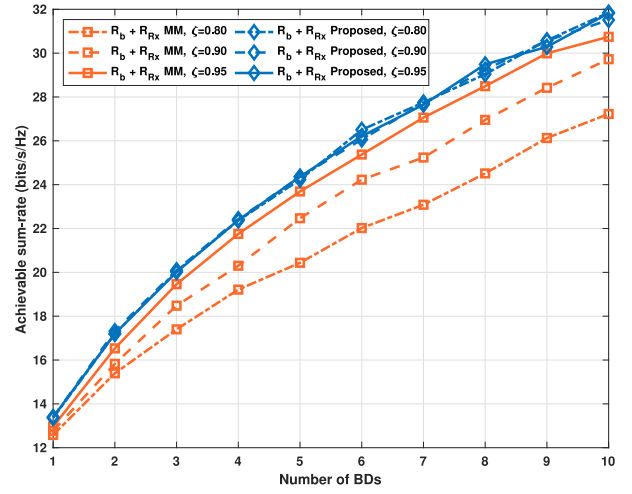

Fig. 2. Achievable sum-rate in SRad system with different number of BDs.

After performing the perfect successive interference cancellation of Rx signal $\mathbf{x}$, the sum-rate of the b-th BD can be measured as

$$R_b = \log_2(1 + \text{SINR}_b), \quad (20)$$

where signal to interference-plus noise-ratio SINR_b at b-th BD can be described as

$$\text{SINR}_b = \frac{\frac{\rho|\beta|^2}{N_p} |\mathbf{f}_{Rx,p|b}^H \mathbf{h}_{Rx,p|b} \Delta_{p|b} \mathbf{h}_{Tx,p|b}^H \mathbf{f}_{Tx,p|b}|^2}{\frac{\rho|\beta|^2}{N_p} \sum_{m \neq (p|b)} |\mathbf{f}_{Rx,m}^H \mathbf{h}_{Rx,p} \Delta_m \mathbf{h}_{Tx,p}^H \mathbf{f}_{Tx,m}|^2 + \sigma_n^2}. \quad (21)$$

IV. SIMULATION RESULTS AND DISCUSSIONS

We consider the following set of parameters for the simulations: $N_{Tx} = 256$, $N_{Rx} = 16$, $N_s = N_p = 4$. The path gains $|\alpha_b|^2$ and $|\alpha_l|^2$ are considered to be between -5dB to -10dB for single bounce paths [12]. Furthermore, we assume $\Gamma_b = 0.1$ when the BD is in non-reflecting state and $\Gamma_b = 0.9$ when BD is in reflecting state.

Figure 2 compares the achievable sum-rate of the symbiotic radio system versus the number of BDs for the proposed signal accessibility scheme and the benchmark MM beam-selection scheme. We consider three values of $\zeta = \{0.80, 0.90, 0.95\}$ for comparison as the value of ζ is selected close to 1 to capture most of the channel power [12]. It is observed from the results of Fig. 2 that the sum-rate of the SRad changes significantly with the change in the value of ζ and number of BDs with the application of benchmark MM scheme. However, the proposed scheme achieves a higher sum-rate compared to the benchmark. Furthermore, the proposed scheme sustains similar performance at different values of ζ. This performance sustainability results from signal accessibility to BDs without signals. Another point to be noted is that in the benchmark scheme, as the ζ value increases, more BDs get access to RF signals; consequently, the number of RF chains also increases.

Figure 3 shows the achievable sum-rate versus signal-to-noise ration (SNR) for $N_b = 1$ and different values $N_l = \{1, 2, 3\}$ and $\Gamma_b = \{0.1, 0.9\}$. The number of selected beams at Tx and Rx are according to N_b and N_l in each case. It is shown that the value of R_{Rx} is maximum when $N_l = 3$
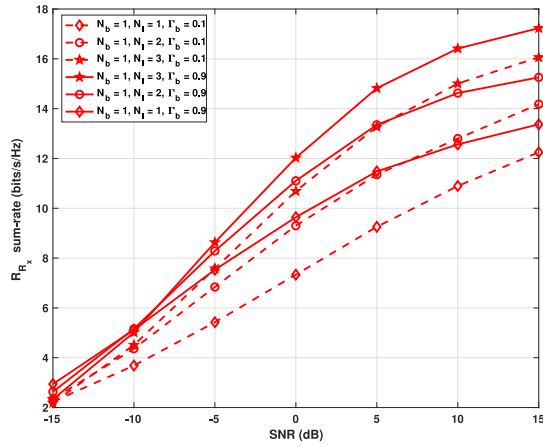
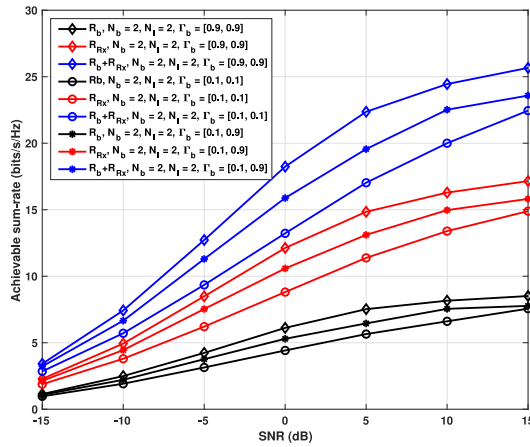Fig. 3. R_{R_x} sum-rate vs SNR for single BD and multiple ordinary scatterers.

Fig. 4. Achievable sum-rate vs SNR for multiple BDs and multiple ordinary scatterers.

and $\Gamma_b = 0.9$. For instance, at 10 dB of SNR, R_{Rx} is around 16 bits/sec/Hz when $N_b = 1, N_l = 3, \Gamma_b = 0.9$ but it drops to 15 bits/sec/Hz when $\Gamma_b = 0.1$. R_{Rx} also decreases with the decreasing value of N_l; for example, it reduces to 11 bits/sec/Hz with $N_l = 1$ and $\Gamma_b = 0.1$. Although changing the value of Γ_b affects R_{Rx}; during the beam-selection through the proposed signal accessibility scheme, we consider maximum reflection $\Gamma_b = 1$ at all BDs.

Figure 4 shows the achievable sum-rate of SRad system with multiple BDs and ordinary scatterers. The sum-rate is obtained with different values of N_b, and N_l. For example, at the SNR value of 10 dB, the highest values of R_b, R_{Rx} and $R_b + R_{Rx}$ are achieved when $N_b = N_l = 2$, and all BDs transmit with the maximum reflection coefficient $\Gamma_b = [0.9, 0.9]$. As one BD reflects with low reflection coefficient, i.e., $\Gamma_b = [0.1, 0.9]$, the sum-rate decreases and it reaches to minimum when both BDs backscatter with minimum $\Gamma_b = [0.1, 0.1]$. Furthermore, Fig. 4 shows that BDs with $\Gamma_b = [0.9, 0.9]$ improve the achievable sum-rate of the system up to 30% compared to BDs with $\Gamma = [0.1, 0.1]$. Thus, simulation results validate the sum-rate enhancement with the beam-selection and also the selection of the paths with different type of scatterers such as BD and ordinary scatterers in the environment.

V. CONCLUSION

In this letter, we proposed a beam selection scheme to maximize the RF signal accessibility to backscatter devices in the mmWave SRad system. As the AmBC system relies on the signals of ambient RF sources, resource availability is crucial for such a system to operate. Due to the sparsity of the mmWave channel, the incident signal may be inaccessible to BDs for communication. Therefore, beams selection in the beamspace domain is performed based on the MM of the channel and choosing the dominant paths between Tx and Rx while ensuring the signal accessibility to BDs. The performance of the beam selection scheme is measured in terms of the achievable sum-rate of the system. The simulation results validate that when beams are selected considering the presence of BDs, it results in sum-rate enhancement of the overall system. Future studies may consider the interference issues when the same beam is selected for multiple BDs.

REFERENCES

[1] L. Zhang, Y.-C. Liang, and M. Xiao, "Spectrum sharing for Internet of Things: A survey," *IEEE Wireless Commun.*, vol. 26, no. 3, pp. 132–139, Jun. 2019.
[2] M. Maier, A. Ebrahimzadeh, S. Rostami, and A. Beniiche, "The Internet of no Things: Making the Internet disappear and 'see the invisible'" *IEEE Commun. Mag.*, vol. 58, no. 11, pp. 76–82, Nov. 2020.
[3] I. F. Akyildiz, A. Kak, and S. Nie, "6G and beyond: The future of wireless communications systems," *IEEE Access*, vol. 8, pp. 133995–134030, 2020.
[4] M. B. Janjua and H. Arslan, "Survey on symbiotic radio: A paradigm shift in spectrum sharing and coexistence," 2021, *arXiv:2111.08948*.
[5] A. Sayeed and J. Brady, "Beamspace MIMO for high-dimensional multiuser communication at millimeter-wave frequencies," in *Proc. IEEE Global Commun. Conf. (GLOBECOM)*, Dec. 2013, pp. 3679–3684.
[6] P. V. Amadori and C. Masouros, "Low RF-complexity millimeter-wave beamspace-MIMO systems by beam selection," *IEEE Trans. Commun.*, vol. 63, no. 6, pp. 2212–2223, Jun. 2015.
[7] G. Yang, T. Wei, and Y.-C. Liang, "Joint hybrid and passive beamforming for millimeter wave symbiotic radio systems," *IEEE Wireless Commun. Lett.*, vol. 10, no. 10, pp. 2294–2298, Oct. 2021.
[8] J. Brady, N. Behdad, and A. M. Sayeed, "Beamspace MIMO for millimeter-wave communications: System architecture, modeling, analysis, and measurements," *IEEE Trans. Antennas Propag.*, vol. 61, no. 7, pp. 3814–3827, Jul. 2013.
[9] T. S. Rappaport et al., "Millimeter wave mobile communications for 5G cellular: It will work!" *IEEE Access*, vol. 1, pp. 335–349, 2013.
[10] O. El Ayach, S. Rajagopal, S. Abu-Surra, Z. Pi, and R. W. Heath, "Spatially sparse precoding in millimeter wave MIMO systems," *IEEE Trans. Wireless Commun.*, vol. 13, no. 3, pp. 1499–1513, Mar. 2014.
[11] B. He and H. Jafarkhani, "Low-complexity reconfigurable MIMO for millimeter wave communications," *IEEE Trans. Commun.*, vol. 66, no. 11, pp. 5278–5291, Nov. 2018.
[12] G. H. Song, J. Brady, and A. Sayeed, "Beamspace MIMO transceivers for low-complexity and near-optimal communication at mm-wave frequencies," in *Proc. IEEE Int. Conf. Acoust. Speech Signal Process.*, May 2013, pp. 4394–4398.
[13] B. Clerckx, Z. B. Zawawi, and K. Huang, "Wirelessly powered backscatter communications: Waveform design and SNR-energy tradeoff," *IEEE Commun. Lett.*, vol. 21, no. 10, pp. 2234–2237, Oct. 2017.
[14] R. W. Heath, N. González-Prelcic, S. Rangan, W. Roh, and A. M. Sayeed, "An overview of signal processing techniques for millimeter wave MIMO systems," *IEEE J. Sel. Topics Signal Process.*, vol. 10, no. 3, pp. 436–453, Apr. 2016.
[15] K. Ardah, S. Gherekhloo, A. L. de Almeida, and M. Haardt, "TRICE: A channel estimation framework for RIS-aided millimeter-wave MIMO systems," *IEEE Signal Process. Lett.*, vol. 28, pp. 513–517, Feb. 2021, doi: 10.1109/LSP.2021.3059363.
[16] X. Gao, L. Dai, S. Han, I. Chih-Lin, and R. W. Heath, "Energy-efficient hybrid analog and digital precoding for mmWave MIMO systems with large antenna arrays," *IEEE J. Sel. Areas Commun.*, vol. 34, no. 4, pp. 998–1009, Apr. 2016.